THE SPECTRUM OF STRONTIUM HYDRIDE

By William W. Watson, Yale University
and W. R. Fredrickson, Syracuse University

(Received January 8, 1932)

Abstract

With a metallic strontium arc in a hydrogen atmosphere as a source, high dispersion spectrograms of three groups of bands in the near infrared with main heads at 7020A, 7347A and 7508A have been obtained. Analysis shows that the latter two groups of bands constitute a $^2\Pi \rightarrow {}^2\Sigma$ system with only the (0, 0) and (1, 1) vibrational transitions, while the first group represents a transition from a higher $^2\Sigma$ to the same normal $^2\Sigma$ state. Quantum analyses of the (0, 0) bands give for the normal $^2\Sigma$ state $B_0'' = 3.6198$ and $D_0'' = -1.287 \times 10^{-4}$, $r_0 = 2.16 \times 10^{-8}$ cm. For the $^2\Pi$ state, $A = 299$, $B_{0,-1/2}' = 3.6683$, $D_{0,-1/2}' = -1.33 \times 10^{-4}$, $B_{0,+1/2}' = 3.6787$ and $D_{0,+1/2}' = 1.13 \times 10^{-4}$. The rotational energy constants for the upper $^2\Sigma$ state are $B_0' = 3.8318$ and $D_0' = -1.641 \times 10^{-4}$. The spin doubling constant γ_0 in the normal state is $+0.122$, in the upper $^2\Sigma$ state it is -3.81, while from the Λ-type doubling in the $^2\Pi$ state $p_0 = -3.92$ and $q_0 = -0.398$. The doubling in the $^2\Sigma$, $^2\Sigma$ band is much the largest yet found in bands of this type. From the near equality of the p_0 of the $^2\Pi$ and the γ_0 of the upper $^2\Sigma$ and their close agreement with calculated values, it is to be concluded that these two states stand to each other in the relation of "pure precession", as is the case for the corresponding states of CaH. The probable electron configurations are then $\cdots 5p\pi$ and $\cdots 5p\sigma$ for the $^2\Pi$ and upper $^2\Sigma$ states and $\cdots 4d\sigma$ for the normal state.

Introduction

Because of the great similarity in the character and relative positions of the lowest levels of the Sr and Ca atoms, one would expect that the band spectra of the SrH and CaH molecules should be somewhat alike. The $^2\Pi \rightarrow {}^2\Sigma$ and $^2\Sigma \rightarrow {}^2\Sigma$ band systems of the CaH molecule show several interesting features because of the large interaction between the $^2\Pi$ and the upper $^2\Sigma$ states.[1] These two states lie but 1320 cm^{-1} apart, and from the magnitude of the observed doublings the amount of l-uncoupling is calculated to be very considerable, the component ρ of l along the direction of the rotational quantum number K being about 0.25 ($l = 1$) when $K = 33$. In view of the "pure precession" relation existing between these states, Mulliken and Christy conclude that the electron configurations are $\cdots 4\,p\pi$ and $\cdots 4\,p\sigma$ for the $^2\Pi$ and upper $^2\Sigma$ states respectively. This makes it possible that the normal $^2\Sigma$ state of CaH is $\cdots 3\,d\sigma$, since in the Ca atom the $3d$ electron is almost as firmly bound as the $4p$. In the Sr atom the $4d$ electron is also almost as firmly bound as the $5p$, with the energy difference even a little smaller than for Ca.

Since the $5^1S - 5^3P_1$ intersystem line for Sr is at 6892A, whereas the corresponding transition for Ca is at 6572A, we could predict that these SrH band systems were to be found in the red region of the spectrum, probably beyond 6900A. Their description, together with the analysis of the BaH

[1] R. S. Mulliken and A. Christy, Phys. Rev. **38**, 87 (1931).

bands given in the preceding paper, completes the body of data on the prominent band systems of the diatomic hydrides of all the elements in the second column of the periodic table.

Experimental Procedure

Practically the same experimental technique was employed in obtaining these SrH spectrograms as has been already described for the case of BaH. The only innovation was in the construction of the electrodes, and was due to the fact that the strontium metal was in the form of rather elongated crystals. Portions of these crystals were broken off, dipped in kerosene, and formed under high pressure into a small solid cylinder of the proper size with a stud protruding from one of its two flat surfaces. This stud of the metal was then made a rivet holding the Sr block on the flattened end of a length of $\frac{1}{8}''$ brass rod which fitted into one of the plugs of the arc chamber. From 10 to 20 of these small Sr electrodes had to be burned in the arc for each exposure.

The band spectra emitted by this arc consist principally of three groups of bands with main heads at 7020A, 7347A and 7508A, degrading toward the violet. The first group and the short wave-length half of the middle group were registered nicely on an Eastman 40 plate dyed with dicyanine. But even though the dicyanine has appreciable sensitivity out to beyond the SrH band line of longest wave-length at 7650A, this sensitivity proved insufficient to give an intense enough spectrogram of this long wave-length end with rather long exposure times. We noted that kryptocyanine has the maximum of its sensitivity curve at about 7500A, however, and with Eastman 40 plates dyed with kryptocyanine we obtained fairly intense spectrograms of this long wave-length portion of the spectrum. In addition to these bands in the red, there is a very dense grouping of lines in the yellow-green region which we have not investigated, and a rather intense small group of bands at 5800A which probably originate in some polyatomic molecule.

Before the measuring of the spectrograms of the red bands, it was observed that the groups at 7347A and 7508A had about the expected spacing and structural features of a $^2\Pi \rightarrow {}^2\Sigma$ system for SrH. The quantum analysis verified this tentative conclusion. With the aid of the combination differences for the $^2\Sigma$ state from this analysis, it was then possible to analyze the 7020A band and to show that it is the predicted $^2\Sigma \rightarrow {}^2\Sigma$ transition with the same lower state as the other system. Fig. 1 is a reproduction of the spectrograms showing these two SrH band systems.

Analysis of the $^2\Pi \rightarrow {}^2\Sigma$ (0, 0) Band

Guided by the intensity distribution among the lines of the 7508A band, and a rough idea of the probable magnitude of the spin doubling in the lower state, the assignment of lines and J values in the P_1, $^PQ_{12}$, Q_1 and $^QR_{12}$ branches proved to be a simple task. The proper designation of R_1 branch lines then followed from the combination differences between the other five branches of this group. The rather peculiar regularity of the spacing of the band lines to the long wave-length side of the $^2\Pi_{1/2}$ origin to be seen in Fig. 1

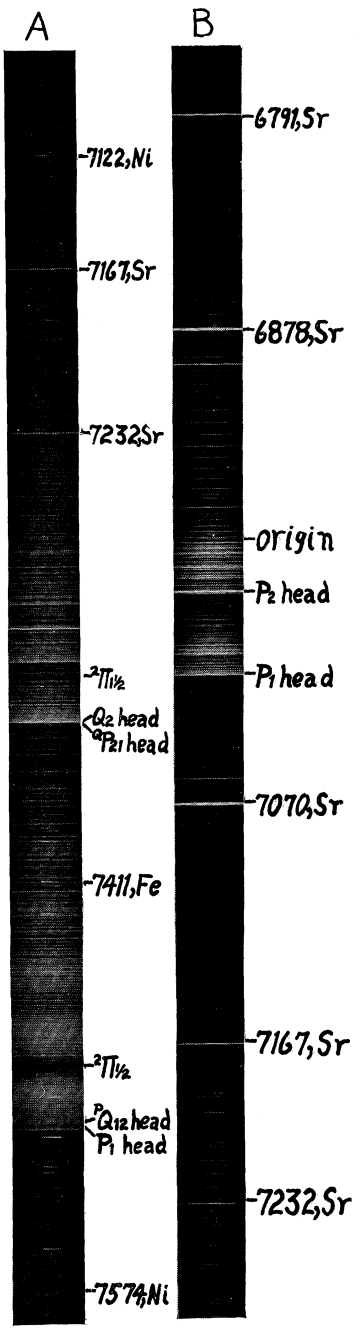

Fig. 1. Reproductions of spectrograms showing the SrH bands. *A*. $^2\Pi \rightarrow {}^2\Sigma$ band sequence. The $^0P_{12}$ branch proceeds out beyond the P_1 head, but the lines are of low intensity. The P_2 branch proceeds similarly towards longer wave-lengths from the Q_2 head, and does not form a head. The head just on the short wave-length side of the $^2\Pi_{1\ 1/2}$ origin belongs to the Q_2 branch of the (1, 1) band. *B*. $^2\Sigma \rightarrow {}^2\Sigma$ band sequence. Note that the head next to the P_1 head is not the P_2 head but rather is P_1 for the (1, 1) band. The large separation of the P_1 and P_2 heads is indicative of the record size of the doubling in the upper $^2\Sigma$ state.

is due to the interlacing of the P_1 and ${}^{P}Q_{12}$ branches. The double-headed appearance of the bands is not as evident as in the case of the BaH system because of the fact that these branches do not turn back.

In the 7347A group of branches the two strong heads would appear to belong to the P_2 and Q_2 branches respectively. But the relative distribution and form of the six branches in each sub-group of a ${}^2\Pi \rightarrow {}^2\Sigma$ band are always similar, and it was therefore concluded that the Q_2 branch produces the first head, the second being due to the Q_2 branch of the (1, 1) band. This arrangement proved to be correct, and with the aid of the various combination differ-

TABLE I. *Assignment of frequencies (cm^{-1}) for (0, 0) band of ${}^2\Pi \rightarrow {}^2\Sigma$ system of SrH (d indicates a double line).*

	${}^2\Pi_{\frac{1}{2}} \rightarrow {}^2\Sigma$					
$J''+\frac{1}{2}$	${}^{O}P_{12}$	P_1	${}^{P}Q_{12}$	Q_1	${}^{Q}R_{12}$	R_1
1			13357.77	13360.87	13362.50*d*	13377.83*d*
2	13339.43*d*	13357.64	56.36	62.50*d*	64.53	90.83
3	26.43*d*	56.07	55.00	64.23	66.50	404.07
4	13.84	54.59	53.70	66.07	68.54	17.27
5	01.31	53.13	52.45	68.01	70.66	30.25
6	288.91	51.76	51.23	70.05	73.03	43.47
7	76.65	50.44	50.07	72.17	75.33	56.56
8	64.52	49.10	48.94	74.42	77.83	69.64
9	52.58	47.85*d*	47.85*d*	76.77	80.36	82.66
10	40.73	46.64*d*	46.64*d*	79.24	83.13	495.69*d*
11	29.11	45.45	45.61	81.80	85.94	508.67*d*
12	17.71	44.24	44.57	84.52	88.95	21.41
13	206.46	43.03	43.48	87.38	91.99	34.20
14	195.40	41.83	42.40	90.41	95.20	46.93
15	84.56	40.66	41.32	93.46	398.58	59.53
16	73.99	39.43	40.22	396.76	402.09	72.00
17	63.62	38.20	39.13	400.09	05.71	84.38
18	53.48	36.94*d*	38.03	03.59	09.48	596.64
19	43.60	35.73*d*	36.94*dd*	07.27	13.39	608.75*d*
20	34.00	34.52*d*	35.73*d*	11.05	17.41	20.82
21	24.65	33.29*d*	34.52*d*	14.99	21.64	32.67
22	15.46	32.02	33.29*d*	19.07	25.94	44.40
23	106.72	30.72	32.14	23.30	30.40	55.94*d*
24	098.18	29.45	31.04	27.69	35.08	67.45
25	089.86	28.12	29.84	32.25	39.86	78.73
26		26.88	28.66	36.96	44.78	689.97
27		25.56	27.53	41.68	49.83	701.12
28		24.34*d*	26.43*d*	46.67	55.07	12.05
29		23.16	25.39	51.79	60.43	23.02
30		21.99	24.34*d*	57.03	65.98	
31		20.90*d*	23.32	62.49	71.59	
32		19.83	22.44	68.04	77.41	
33		18.86	21.78	73.79	83.37	
34		17.97	29.90*d*	79.67	89.50	
35		17.21	20.40	85.65	495.69	
36		16.50		91.95*d*	502.18	
37		15.92		498.20	08.67	
38		15.48		504.64	15.48	
39		15.24		11.28	22.29	
40				18.04	29.22	
41				24.99	36.23	
42				32.05		
43				39.24		
44				46.58		
45				54.07		
46				61.66		

TABLE I. (*Continued*).

	$^2\Pi_{1\frac{1}{2}} \rightarrow {}^2\Sigma$					
$J''+\frac{1}{2}$	P_2	$^QP_{21}$	Q_2	$^RQ_{21}$	R_2	$^SR_{21}$
2			13644.83	13659.27	13663.12	13677.59
3	13622.66	13644.39	41.52	62.90	67.26	88.67
4	12.31	41.04	38.25	66.73	71.21	699.99*d*
5	601.89	37.64	35.10	70.68	75.32	711.26
6	591.53	34.53*d*	32.10	74.57	79.52	22.67
7	81.18	31.26	29.20	78.73	83.75	34.14
8	70.98	28.20	26.44	82.84	88.04	45.59*d*
9	60.91	25.36	23.87	86.98	92.44	57.03
10	51.00	22.66	21.28	91.23	696.86	69.18
11	41.09	20.06	19.06	95.57	701.38	81.13
12	31.41	17.66	16.97	699.99*d*	06.02	793.19
13	21.87	15.50	15.04	704.43	10.63	804.89
14	12.44	13.33*d*	13.33*d*	08.98	15.35	17.61
15	503.28	11.66	11.80	13.62	20.19	29.95
16	494.18	09.59	10.58	18.31	25.11	42.58
17	85.21	08.75*d*	09.59	23.02	30.09	55.25
18	76.56	07.39	08.75	27.94	35.15	68.11
19	68.04	06.53	08.16	32.88	40.28	81.09
20	59.70	05.87	07.92	37.90	45.59*d*	894.32
21	51.69	05.44	07.92	43.06	50.85	907.60
22	43.69	05.44	08.16	48.22	56.27	21.11
23	36.06	05.44	08.75	53.60	61.71	34.75
24	28.61		09.59	58.98	67.38	48.70
25	21.07		10.87	64.53	73.06	62.48
26	13.65		12.31	70.14	78.87	76.44
27	406.37		14.05	75.77	84.85	13990.79
28	399.25		16.11	81.68	90.79	14005.19
29			18.47	87.60	796.98	19.62
30			21.12	93.63	803.21	34.26
31			23.96	799.77	09.53	48.98
32			27.24	806.08	16.09	63.86
33			30.74	12.34	22.67	78.79
34			34.53	18.91	29.29	093.71
35			38.61	25.50	36.14	108.83
36			42.96	32.22	43.04	23.93
37			47.55	39.11	50.08	
38			52.51	46.15	57.08	
39			57.49	53.20		

ences mentioned in the discussion of the BaH spectrum, the assignments to the other branches were made. The wave numbers of all the lines of the twelve branches of this SrH band are given in Table I.

Fortrat diagrams of these $^2\Pi \rightarrow {}^2\Sigma$ bands of BaH and SrH of course show considerable similarity since the ratio A/B is somewhat the same for both. The most evident difference between the two is that the Q_1 branch lies much nearer to the P_1 branch than to the R_1 branch in the SrH diagram, whereas in the case of BaH the Q_1 branch is rather nearer the R_1 branch. This difference in the relative position of the Q_1 branch is due to the fact that the large Λ-type doubling in the $^2\Pi_{1/2}$ state is of opposite sign in the two bands.

EVALUATION OF THE CONSTANTS B, D AND A

The lower state combinations defined by Eq. (1) of the preceding paper from which the molecular constants are computed are listed in Table II. The last column of this table gives the average values from which the B_0'' and D_0'' given in Table IV were calculated from Eq. (3) of the BaH paper.

TABLE II. *Lower state combinations.* The 1st set of data gives the Δ_2F_1'' values obtained from Eq. (1) of preceding paper. The second set the $\Delta_2F_2''(J)$. The J values have been omitted in headings; $R_1-P_1=R_1(J-1)-P_1(J+1)$, etc. The $\Delta_2F''(K)$ values in the last column are the average of $\Delta_2F_1''(J=K+\frac{1}{2})$ and $\Delta_2F_2''(J=K-\frac{1}{2})$, used in Eq. (3).

	$\Delta_2F_1''(J)$				$\Delta_2F_2''(J)$				
$J''+\frac{1}{2}$	R_1-P_1	${}^SR_{21}-{}^QP_{21}$	av.	$J''+\frac{1}{2}$	R_2-P_2	${}^QR_{12}-{}^QP_{12}$	av.	K	$\Delta_2F''(K)$
2	21.76		21.76	2		36.07	36.07	1	21.76
3	36.24	36.55	36.40	3	50.81	50.69	50.75	2	36.15
4	50.94	51.03	50.98	4	65.37	65.19	65.28	3	50.81
5	65.51	65.46	65.49	5	79.68	79.63	79.65	4	65.36
6	79.81	80.00	79.90	6	94.14	94.01	94.07	6	79.71
7	94.37	94.47	94.42	7	108.54	108.51	108.52	6	94.25
8	108.71	108.78	108.75	8	122.84	122.75	122.80	7	108.62
9	123.00	122.93	122.96	9	137.04	137.10	137.07	8	122.62
10	137.21	136.97	137.09	10	151.35	151.25	151.30	9	137.08
11	151.45	151.52	151.49	11	165.45	165.42	165.43	10	151.39
12	165.64	165.63	165.63	12	179.51	179.48	179.50	11	165.53
13	179.58	179.86	179.72	13	193.58	193.55	193.56	12	179.60
14	193.54	193.23	193.38	14	207.35	207.43	207.39	13	193.47
15	207.50	208.02	207.76	15	221.17	221.21	221.19	14	207.43
16	221.33	221.20	221.27	16	234.98	234.96	234.97	15	221.24
17	235.06	235.19	235.12	17	248.55	248.61	248.58	16	235.00
18	248.65	248.72	248.68	18	262.05	262.11	262.08	17	248.60
19	262.12	262.24	262.18	19	275.45	275.48	275.46	18	262.09
20	275.46	275.65	275.55	20	288.59	288.74	288.67	19	275.46
21	288.80	288.88	288.84	21	301.90	301.95	301.92	20	288.73
22	301.95	302.16	302.05	22	314.79	314.92	314.85	21	301.93
23	314.99		314.99	23	327.66	327.76	327.71	22	314.90
24	327.82		327.82	24	340.64	340.54	340.59	23	327.75
								24	340.59

TABLE III. *Upper state combinations.* The Δ_2F'' headings are defined by Eq. (2) in preceding paper. $\Delta_2F_{1dc}(J)$ is the average of $\Delta_2F_{1c}(J)$ and $\Delta_2F_{1d}(J)$. $\Delta_2F_{2dc}(J)$ is the average of $\Delta_2F_{2d}(J)$, and $\Delta_2F_{2c}(J)$.

$J''+\frac{1}{2}$	$\Delta_2F_{1d}(J)$	$\Delta_2F_{1c}(J)$	$\Delta_2F_{1dc}(J)$	$J''+\frac{1}{2}$	$\Delta_2F_{2d}(J)$	$\Delta_2F_{2c}(J)$	$\Delta_2F_{2dc}(J)$
2	33.19	25.10	29.15	2			
3	48.00	40.07	44.03	3	44.60		44.60
4	62.68	54.70	58.69	4	58.90	58.95	58.93
5	77.12	69.35	73.24	5	73.43	73.62	73.52
6	91.71	84.12	87.41	6	87.99	88.14	88.07
7	106.12	98.68	102.40	7	102.57	102.88	102.72
8	120.54	113.31	116.93	8	117.06	117.39	117.23
9	134.81	127.78	131.30	9	131.53	131.67	131.60
10	149.05	142.40	145.72	10	145.86	145.52	146.19
11	163.22	156.83	160.02	11	160.29	161.07	160.78
12	177.17	171.24	174.21	12	174.61	175.53	175.07
13	191.17	185.53	188.35	13	188.76	189.39	189.08
14	205.12	199.80	202.46	14	202.91	204.28	203.60
15	218.87	214.02	216.45	15	216.91	218.29	217.60
16	232.57	228.10	230.33	16	230.93	232.99	231.96
17	246.18	242.09	244.14	17	244.88	246.50	245.69
18	259.70	256.00	257.85	18	258.59	260.72	259.66
19	273.02	269.79	271.40	19	272.24	274.56	273.40
20	286.30	283.41	284.86	20	285.89	288.45	287.17
21	299.38	296.99	298.18	21	299.16	302.16	300.66
22	312.38	310.48	311.43	22	312.58	315.67	314.12
23	325.22	323.68	324.45	23	325.65	329.31	327.48
24		336.90		24	338.77		
25		350.00		25	351.99		

This value of $B_0''=3.6198$ corresponds to an internuclear distance of 2.16×10^{-8} cm. Table III contains the combinations as defined by Eq. (2) for the

$^2\Pi$ state. Again the average values listed in the columns headed $\Delta_2F_{dc}(J)$ and defined by Eq. (4) were used in calculating the B_0' and D_0' constants.[2] These constants are given in Table IV.

Calculation of the coupling constant A for the $\Lambda\Sigma$ interaction using the Hill and Van Vleck equation gives $A=299$. This value stands to the coupling

TABLE IV. *Constants from the quantum analysis of the SrH bands (cm^{-1} units).*

Normal $^2\Sigma$ state:	$B_0''=3.6198$, $D_0''=-1.287\times10^{-4}$, $r_0=2.16\times10^{-8}$ cm
	$\gamma_0=+0.122$
$^2\Pi$ state:	$B_{0,-1/2}'=3.6683$, $D_{0,-1/2}'=-1.33\times10^{-4}$
	$B_{0,+1/2}'=3.6787$, $D_{0,+1/2}'=1.13\times10^{-4}$
	$A=299$, $p_0=-3.92$, $q_0=-0.398$
Upper $^2\Sigma$ state:	$B_0'=3.8318$, $D_0'=-1.641\times10^{-4}$, $\gamma_0'=-3.81$

constant $A=387$ for the lowest ^3P state of the strontium atom in practically the same ratio as exists between the A's for the corresponding $^2\Pi$ state of CaH and the lowest ^3P state of Ca.

ANALYSIS OF THE 7020A $^2\Sigma\rightarrow{}^2\Sigma$ (0, 0) BAND OF SrH

There are eight series of lines or branches in the 7020A band, four of which belong to the (0,0) and the other four to the (1, 1) vibrational transition. Assuming that the branch forming the first head on the red end is the P_1 of the (0, 0) band, that series which with this P_1 branch gives the same lower state combinations $\Delta_2F_1''(J)$ as previously found for the $^2\Pi\rightarrow{}^2\Sigma$ band was designated as the corresponding R_1 branch. Then knowing exactly the doubling in the normal $^2\Sigma$ state, those two of the remaining six series which give the same $\Delta_2F_2''(J)$ combination differences as found above for the $^2\Pi\rightarrow{}^2\Sigma$ band could be labelled the P_2 and R_2 branches. The assignment of wave numbers for these four branches is given in Table V. The R_2 branch is relatively quite weak, and we can follow it only to $J=15\frac{1}{2}$ on our spectrograms. This may be due to the fact that the sensitivity of the dicyanine dye is beginning to decrease a little in this wave-length region.

The second head of this 7020A band to be seen in Fig. 1 is not formed by the P_2 branch, as one would at first suppose, but is rather the P_1 head of the (1, 1) band. The large separation of the P_1 and P_2 branch heads indicates a very large spin doubling in the upper $^2\Sigma$ state (cf. next section). Providing the doubling in both of the electronic states involved is sufficiently large, weak Q_{21} and Q_{12} branch lines are expected near the origin as satellites of the P and R lines in bands of this type. The evidence for their existence in this band is not very good, however. There is a line that could be designated $Q_{21}(\frac{1}{2})$ about 6 cm^{-1} to the high frequency side of $R_1(\frac{1}{2})$ as it should be, but it is obviously a double or triple line. The other Q_{21} and Q_{12} lines are probably too close to the R_2 and P_1 lines respectively to be resolved on our spectrograms.

Table VI contains the lower state combination differences for this band. The values are practically identical with those of the $^2\Pi\rightarrow{}^2\Sigma$ band given in

[2] Evaluation of $B_{0,-1/2}'$ from the Δ_2F_{1c} and Δ_2F_{1d} values separately gives $B_{0,-1/2,c}'=3.5206$ and $B_{0,+1/2,d}'=3.8231$.

TABLE V. *Assignment of frequencies for the 7020A $^2\Sigma \rightarrow {}^2\Sigma$ (0, 0) band of SrH (d indicates a double line; cm^{-1} units).*

$J+\frac{1}{2}$	P_1	R_1	P_2	R_2
1		14357.81		14373.71*d*
2	14345.30	363.79		384.20*d*
3	336.01	370.78	14337.52	395.00*d*
4	327.14	376.93	333.74*d*	406.30
5	319.60	384.20	329.95	417.83
6	311.54	391.73	326.66	429.66
7	304.31	399.71	323.75	441.86
8	297.44	408.03	321.19	454.37
9	290.92	416.79	319.00	467.12
10	285.01	425.90	317.28	480.17
11	279.45	435.26	315.85	493.48
12	274.35	445.08	314.80	507.06
13	269.63	455.24	314.25	520.83
14	265.32	465.72	313.82	534.90
15	261.52	476.50	313.47	548.76
16	258.06	487.62	313.82	563.45
17	255.04	498.99	314.25	
18	252.35	510.64	314.80	
19	250.22	522.64	314.80	
20	248.45	534.80	315.85	
21	247.03	547.29	317.28	
22	246.00	559.98	319.06	
23	245.27	572.90	321.19	
24	244.99	586.03	323.77	
25	244.99	599.38	326.66	
26	245.27	612.86	329.42	
27	246.00	626.48	332.18	
28	247.03	640.26	335.16	
29	248.45	654.21	338.62	
30	250.23	668.26	342.20	
31	252.35		346.03	
32	254.48		350.20	
33	257.02		354.58	
34	259.86		359.02	
35	262.85		363.79	
36	266.04		368.66	
37	269.63		373.71	
38	273.34		378.90	
39	277.33		384.20	
40	281.41		389.55	
41	285.71		395.00	
42	290.09		400.50	
43	294.46		406.30	
44	299.18		412.17	

Table II, showing that the two systems have the same normal $^2\Sigma$ state. The initial state combinations are given by the relations

$$R_1(J) - P_1(J) = F_1'(J+1) - F_1'(J-1) = \Delta_2 F_1'(J)$$
$$R_2(J) - P_2(J) = F_2'(J+1) - F_2'(J-1) = \Delta_2 F_2'(J).$$

These values are also listed in Table VI. There is a large divergence between the values of $\Delta_2 F_1'$ and $\Delta_2 F_2'$ due to very large spin doubling. In fact this doubling is the largest yet found for any $^2\Sigma$ state. Nevertheless, as in the case of the lower $^2\Sigma$ state, if we represent by $T_1(K)$ the levels with $J=K+\frac{1}{2}$ and by $T_2(K)$ the levels with $J=K-\frac{1}{2}$, then $T'(K)=\frac{1}{2}\{T_1(K)+T_2(K)\}$ has the value

$$T(K) = T_0 + T_v + B'[K(K+1) - G^2] + D'K^2(K+1)^2 + \tfrac{1}{2}\gamma$$

TABLE VI. *Upper and lower state combinations of 7020A* $^2\Sigma \rightarrow {}^2\Sigma$ *band.* The $\Delta_2F(K)$ values are the average of the second and third columns in each set, and are the ΔF values from which the constants are calculated.

Lower state combinations					Upper state combinations				
$J''+\frac{1}{2}$	R_1-P_1	R_2-P_2	K	$\Delta_2F''(K)$	$J+\frac{1}{2}$	$R_1(J)$ $-P_1(J)$	$R_2(J)$ $-P_2(J)$	K	$\Delta_2F(K)$
2	21.80	36.19	1	21.80	2	18.49		1	
3	36.65	50.46	2	36.42	3	34.17	57.48	2	
4	51.12	65.05	3	50.79	4	49.79	72.56	3	53.63
5	65.39	79.64	4	65.22	5	65.14	87.88	4	68.85
6	79.89	94.08	5	79.76	6	80.19	103.00	5	84.04
7	94.29	108.47	6	94.18	7	95.40	118.11	6	99.20
8	108.79	122.86	7	108.63	8	110.59	133.18	7	114.35
9	123.02	137.09	8	123.94	9	125.87	148.12	8	129.52
10	137.34	151.29	9	137.22	10	140.89	162.89	9	144.51
11	151.55	165.37	10	151.42	11	155.81	177.63	10	159.35
12	165.63	179.23	11	165.50	12	170.73	192.26	11	174.18
13	179.76	193.24	12	179.50	13	185.61	206.58	12	188.94
14	193.72	207.36	13	193.48	14	200.40	221.08	13	203.49
15	207.66	221.08	14	207.51	15	214.98	235.29	14	218.03
16	221.46	234.51	15	221.27	16	229.56	249.63	15	232.42
17	235.27	248.65	16	234.89	17	243.95			
18	248.77		17	248.71	18	258.29			
19	262.19				19	272.42			
20	275.61				20	286.35			
21	288.80				21	300.26			
22	302.02				22	313.98			
23	314.99				23	327.63			
24	327.91				24	341.04			
25	340.76				25	354.39			
26	353.38				26	367.59			
27	365.83				27	380.48			
28	378.03				28	393.23			
29	390.03				29	405.76			
30	401.86				30	418.03			
31	413.78								

and

$$\Delta_2F'(K) = B'(4K + 2) + D'(8K^3 + 12K^2 + 12K + 4).$$

The $\Delta_2F'(K)$ values are given in the last column of Table VI. These have been used to compute the B_0 and D_0 constants for this upper $^2\Sigma$ state given in Table IV.

SPIN DOUBLING IN THE $^2\Sigma$ STATES AND Λ-TYPE DOUBLING IN THE $^2\Pi$ STATE OF THE SrH BANDS

These bands offer an interesting example, very similar to that of CaH, for the application of the theory of spin and Λ-type doubling. Fig. 2 exhibits the spin doublings in both of the $^2\Sigma$ states of SrH, as well as the Λ-type doubling in the $^2\Pi_{1/2}$ $^2\Pi_{1\,1/2}$ levels. The computations for these curves were carried out in exactly the same way as outlined in the preceding paper, and the values of the doubling constants γ, p, and q given in Table IV have been calculated using equations (5) and (6). The change of slope of the spin doubling curve for the upper $^2\Sigma$ state, just as for the corresponding state of CaH, is probably due to the perturbing effect of other near-lying levels. Fig. 3 shows the relative spacing of the four terms of the $^2\Pi$ states with increasing K, $T_{1d}(J)$ being

taken as zero. Comparing this figure with the corresponding diagram in the preceding paper, we note that the separation of the T_2 levels is greater for SrH than for BaH, indicating that this $^2\Pi$ state of BaH is much closer to case a. The separation of the T_1 levels is greater for SrH than for the corresponding levels of either CaH[1] or BaH because of the large interaction with the near-lying upper $^2\Sigma$ state. But nevertheless these two levels begin to approach each other at $K'=28$, showing that transition towards case b is setting in.

It is to be noted that all the doubling constants except γ_0 for the normal $^2\Sigma$ state are negative. The fact that the p_0 and q_0 of the $^2\Pi$ state are negative

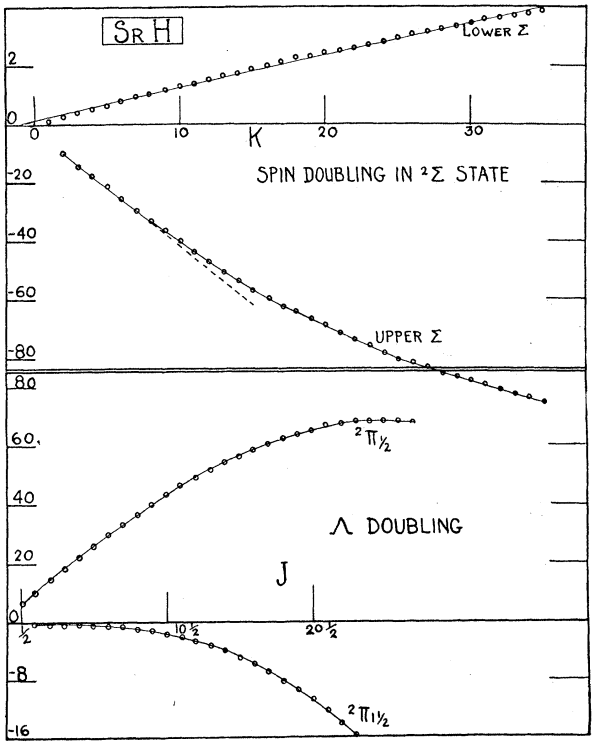

Fig. 2. Spin and Λ-type doublings in the SrH states. Note particularly the change in slope of the spin doubling curve for the upper $^2\Sigma$ state as compared to the usual linear relation holding for the normal $^2\Sigma$ state, and the tendency for the Λ-type doubling in the $^2\Pi_{1/2}$ state to finally begin to decrease as J becomes large showing the setting-in of a transition towards case b.

indicates interaction with a $^2\Sigma^+$ state above it, and that this interaction is with the observed upper $^2\Sigma$ state is attested by the near equality of this $p_0=-3.92$ with the $\gamma_0=-3.81$ for the $^2\Sigma$ state as well as by the size of these quantities. For the similar $^2\Pi$ state of BaH where there is no such near $^2\Sigma$ state above it, we have shown that the constants p_0 and q_0 are positive and much smaller in value. And calculation with the formulas for $\gamma=p$ and for q assuming pure precession between these two SrH states (Equations (8) of the preceding paper), with A and B as given in Table IV, $l=1$, and $\nu(\Pi, \Sigma)$

$= -850$ (the difference in cm^{-1} between the mean of the Π levels and the upper $^2\Sigma$ level), gives $\gamma = p = -5.18$ and $q = -0.63$.

These relations between these SrH states demonstrate that a very considerable amount of l-uncoupling takes place with increase of the molecular rotation, as is also true for the corresponding CaH states.[1,3] Setting the doublet interval of the upper $^2\Sigma$ level equal to $A\rho$, where ρ is the component of l in the direction of K, we compute that at $K = 35$ $\rho = 95/299 = 0.32$. For the $^2\Pi_d$ levels, then, the doublet interval for large K should become much larger than that calculated according to the Hill and Van Vleck equation, while the interval between the $^2\Pi_c$ levels should asymptotically approach zero as K increases.[1] If our data for the doubling in the SrH $^2\Pi$ state extended to higher K

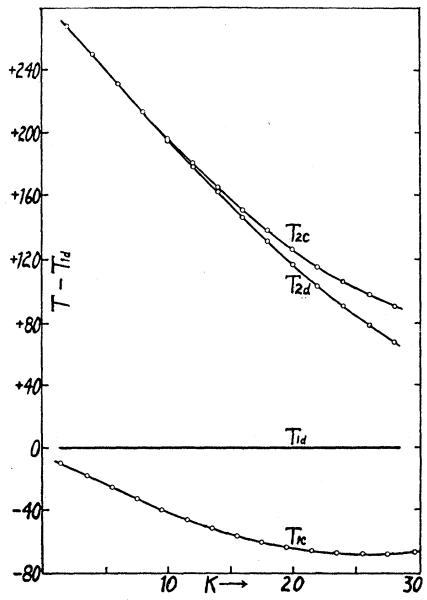

Fig. 3. Relative separations of the term values for the $^2\Pi$ state of SrH, $T_{1d}(J)$ being taken as zero. Compare the similar diagrams for CaH (reference 1) and for BaH (preceding paper).

values, we would expect to see this behavior of the Π levels about as well illustrated as for CaH, for the comparison of our Fig. 3 with the similar plot for CaH[4] shows the same trends occurring with increasing K.

Discussion

In view of the low energy of the lowest ^3D levels in Ca, Sr and Ba and the relative position of this ^3D and the ^3P in these atoms and that of the $^2\Pi$ and upper $^2\Sigma$ states (assuming the indicated BaH band farther into the red to be $^2\Sigma$, $^2\Sigma$) in CaH, SrH and BaH, it is tempting to consider the normal state to be $\cdots np\sigma$ and the upper $^2\Sigma$ to be $\cdots (n-1)d\sigma$. However, the same argu-

[3] W. W. Watson, Phys. Rev. **39**, 278 (1932).
[4] Reference 1, Fig. 4.

ments that led Mulliken and Christy[1] to interpret the upper $^2\Sigma$ state of CaH as $\cdots 4p\sigma$ hold for SrH. For, as we have shown above, the equality of the doubling constants p_0 for the $^2\Pi$ state and γ_0 for the upper $^2\Sigma$ state and their close agreement with the calculated values assuming a relation of pure precession with $l=1$ makes it highly probable that this relation exists between these two states. Therefore these two states are to be considered as $\cdots 5p\pi$ and $\cdots 5p\sigma$ respectively, which leaves $\cdots 4d\sigma$ as the possible electron configuration for the normal $^2\Sigma$ state.

It is necessary to attribute the fact that $np\sigma$ lies above $np\pi$ to a quantum mechanical repulsion between the normal $(n-1)d\sigma$ and the $np\sigma$ states. Also this interpretation predicts a $\cdots (n-1)d\pi$ $^2\Pi$ state which must lie higher than the $\cdots np\pi$, $^2\Pi$ state, for if it were lower the interaction with the normal state would produce a considerably larger γ_0 in the latter than is observed. Possibly there may be bands for CaH and SrH involving this $\cdots (n-1)d\pi$, $^2\Pi$ and a $\cdots (n-1)d\delta$, $^2\Delta$, with perhaps close approach to case d' conditions, and lying farther into the ultraviolet than heretofore investigated. It may be too that the dissociation relations for all these states are complicated, as was suggested in the preceding paper as a really necessary assumption for the BaH states in view of their observed constants.

We wish to thank Dr. Alden J. King for the generous supply of pure strontium metal placed at our disposal, and we are indebted to Professor R. S. Mulliken for helpful correspondence on the subject of the nature of the probable electronic configurations.

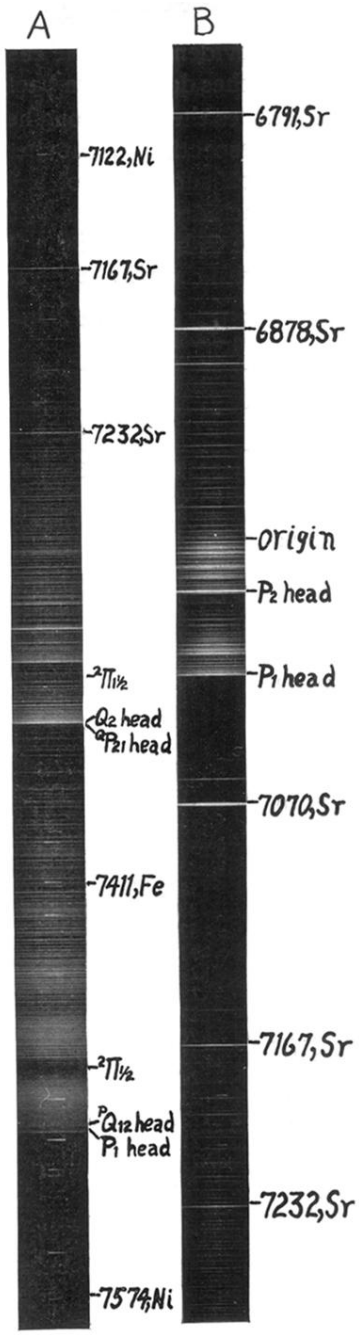

Fig. 1. Reproductions of spectrograms showing the SrH bands. *A*. $^2\Pi \rightarrow {}^2\Sigma$ band sequence. The $^0P_{12}$ branch proceeds out beyond the P_1 head, but the lines are of low intensity. The P_2 branch proceeds similarly towards longer wave-lengths from the Q_2 head, and does not form a head. The head just on the short wave-length side of the $^2\Pi_{1\ 1/2}$ origin belongs to the Q_2 branch of the (1, 1) band. *B*. $^2\Sigma \rightarrow {}^2\Sigma$ band sequence. Note that the head next to the P_1 head is not the P_2 head but rather is P_1 for the (1, 1) band. The large separation of the P_1 and P_2 heads is indicative of the record size of the doubling in the upper $^2\Sigma$ state.